DAMAGE ASSESSMENT IN RAILWAY SUB-STRUCTURES DETERIORATED USING AE TECHNIQUE

Tomoki Shiotani*, Yasuhiro Nakanishi*, Xiu Luo** and Hiroshi Haya**

*Research Institute of Technology, Tobishima Corporation
5472 Kimagase, Noda, Chiba 270-0222, Japan.
**Railway Technical Research Institute
2-8-38 Hikari-machi, Kokubunji, Tokyo 185-0034, Japan.

ABSTRACT

Due to earthquakes, differential settlement and long-term weathering, civil structures have sustained deterioration. In super-structures located above ground, except for seriously damaged structures, evaluation of moderately or intermediately damaged structures is difficult. In sub-structures the damage would not be readily assessed even for severely damaged structures. AE testing has a potential to evaluate thus damages not only for super-structures but sub-structures since it is a monitoring technique to detect fracture-associated elastic waves. In the present paper, damage indices using AE activity is discussed with actually damaged concrete piers. Railway traffic is utilized to induce AE activity. Through in-situ monitoring, it can be concluded that AE monitoring is a promising technique to quantify the damages in the railway structures.

Key words: Calm ratio, damage assessments, railway structures, RTRI, improved *b*-value

1. Introduction

Currently strong movement to make AE monitoring standard in concrete engineering can be seen e.g., in the recommended practice for in-situ monitoring of concrete structures [1]. Since the standard was based on the laboratory studies [2], AE applications in practical however, there are some issues to be resolved. In the present paper, the applicability of AE technique will be discussed with two railway sub-structures, a plain concrete pier and a RC pier both deteriorated. As indices for damage degree, RTRI and Calm ratio as well as improved *b*-value are studied in comparison with actual damage observed.

2. Characteristic AE activity with damage evolution

Under incremental cyclic loads in concrete, AE activity can be represented with damage progress as shown in Fig. 1. Provided that damage levels are classified into four different levels: intact; almost intact; slightly damaged; and heavily damaged, AE activity characterized by each damage level is demonstrated as in the chart. In the second cyclic load, AE activity would start to be observed at the load level of the maximum prior load. This phenomenon is referred to as Kaiser effect. In the subsequent third cyclic load, in which the material shows slightly damaged, the onset of AE appearance would be at a smaller level than previously. Decrease of effective

areas against external load or accumulation of microcracks within materials appears to play significant roles to show the behavior. Considering the relation of AE activity to the stress level experienced, such damage-indices as Felicity ratio [3], CBI ratio [4], and Load ratio [1] have already been proposed. It is also important to pay attention to the AE activity during unloading processes [5]. With damage evolution, not only the AE activity during uploading, but that during unloading would become more intense. Accumulation of shear type of cracks seems to be attributed to this phenomenon. The ratio of accumulated number of AE activity during uploading to that during unloading, is refereed to as Calm ratio [1]

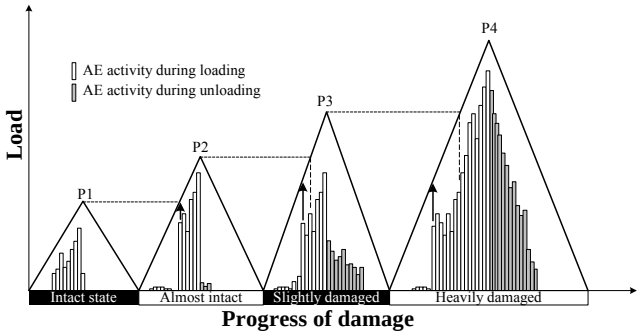

Fig. 1 Representation of AE activity with damage progress.

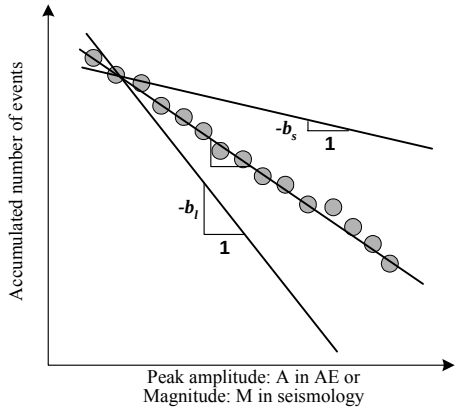

Fig. 2 Peak amplitude distribution

2.1 Damage indices using AE parameters

For the ratios mentioned previously, they may be difficult to apply for in-situ monitoring since the maximum stress of which the materials have experienced is not readily estimated. Thus, the authors have proposed a RTRI ratio instead [6]. The RTRI ratio is defined as in the following procedure: the onset of AE activity is estimated on the basis of whichever measured parameters as stress/load, strain/deformation and so forth; and the ratio is obtained as the ratio of the onset of the AE activity to the maximum value (or peak value) during an inspection period, instead of the maximum stress of which the structure has experienced.

In addition to those indices shown, AE peak amplitudes are also known to be closely related to the scale of fracture, namely degree of damage. Thus, the scale of peak amplitude would be larger with progress of fracture. However, it seems difficult only to pay attention to the peak amplitude. As fracture develops, an apparent mechanical property of the structure would be changed as well, so that condition of media of which AE signals travel would be worse i.e., a high attenuation rate causes the fact that even AE peak amplitude of large scale at the source results in small scale at the sensor. Accordingly, in the present paper the peak amplitudes are going to be studied as their distributions. Many researchers have therefore studied *b*-value and *m*-value determined from a negative gradient of the peak-amplitude distribution (see Fig. 2). To apply the *b*-value analysis for the evaluation of stability in slopes, the method for calculating the *b*-value has been modified by incorporating statistical values of amplitude distribution [7, 8]. This is now referred to as ‘improved *b*-value (I*b*-value) analysis.’

3. In-situ applications

3.1 A concrete pier damaged due to differential settlement (C-pier)

In situ AE monitoring was performed in a pier (h x l x w = 5.5 x 12.3 x 2.6 m) of a railway bridge. The pier was made of plain concrete, and more than 70 years has passed since the construction. During the service, the pier was deteriorated due to differential settlement, and resulting macroscopic shear cracks were found. The crack observed was penetrated, and roughly repaired traces were found along the crack. The monitoring site was located a suburb of Tokyo, and about 420 times train passages a day were repeatedly loaded over the bridge. Crack motions were measured by π-shaped displacement meters. The AE sensors array along the penetrated crack is shown as in Fig. 3 as well as AE sources located. 12 AE sensors with built in preamplifier (R6I, Physical Acoustics Corp.) were firmly fixed onto the pier surface with springs. AE events induced by train passage in service were subsequently amplified by 40 dB at preamplifiers and fed to AE monitoring system (Mistras, Physical Acoustics Corp.) Both, AE parameters and waveforms are recorded with the system.

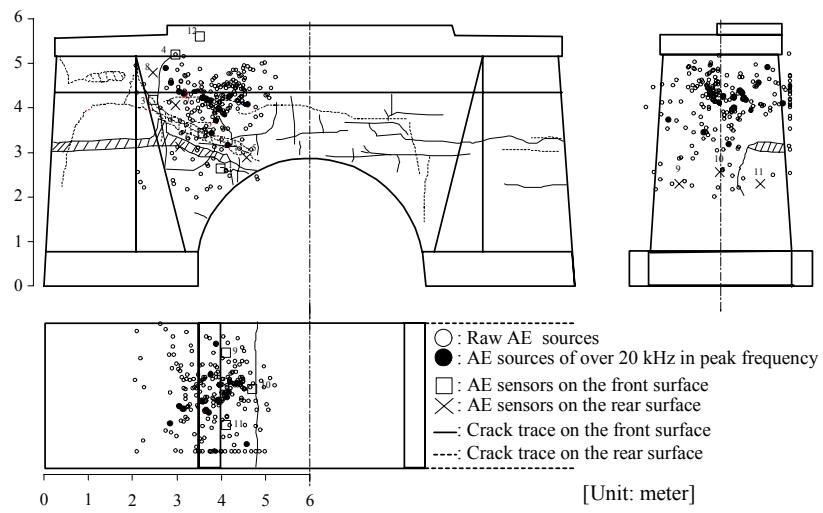

Fig. 3 Arrangement of AE sensors together with 3D AE sources.

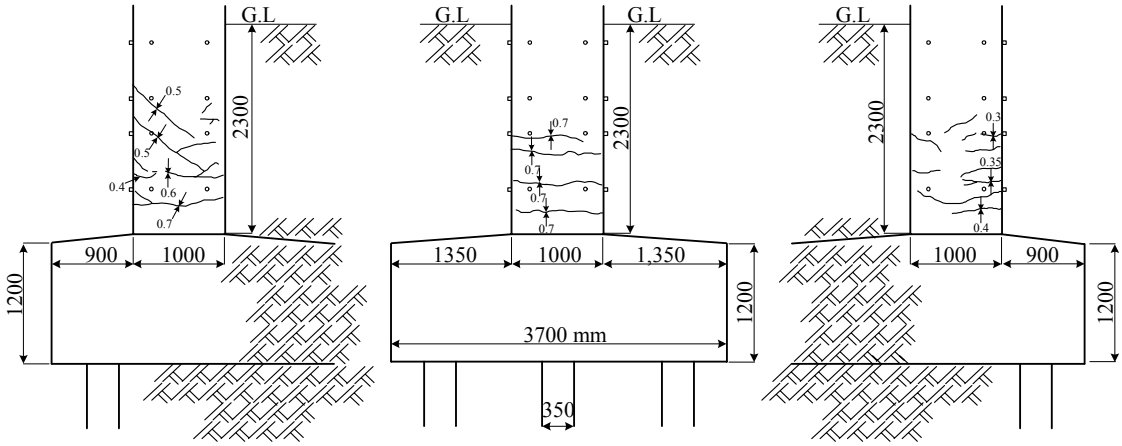

Fig. 4 Crack traces observed in RC-pier, showing north, east and south side from left to right.

3.2 A RC pier damaged by an earthquake (RC-pier)

AE monitoring was conducted in a RC pier of a railway rigid-frame bridge, where a bullet train passes a several times an hour. Due to a great earthquake (M_w=7.0) in 2003, super-structures of almost piers were seriously damaged. In the pier subjected to the monitoring, however, critical cracks were not found above ground but seriously damaged condition was

readily found in the lower part embedded into ground. The crack observed below ground is shown as in Fig. 4. In the north side, for example, a crack of 0.7 mm wide was found just above the footing and a diagonal crack, namely a shear type of crack, was observed at 1 m above the footing. Those cracks principally distributed up to 1.5 m above the footing. To know the AE activity not only for seriously damaged but intermediately damaged state, two arrays of AE sensors, A-array and B-array, were employed as shown in Fig. 5. A-array corresponds to the seriously damaged area while B-array shows the intermediately damaged area. In each array, 12 AE sensors of 60 kHz resonance surrounds the pier. The same AE monitoring system and monitoring condition as those in C-pier was used.

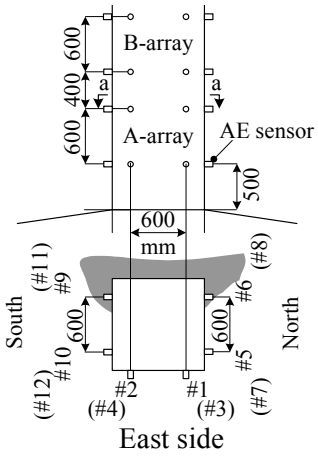

Fig. 5 AE sensor array.

4. Results

4.1 AE sources located

Fig. 3 shows 3D source locations in case of C-pier. The AE sources were induced by train passage in service. The sources are drawn with open circles, in especial solid circles show the sources of more than 20 kHz in peak frequency. The raw AE sources spread over the monitoring area irrespective of the crack location, however, the sources of over 20 kHz were narrowly located along the pre-existing crack. Presumably, the AE sources over 20 kHz are closely related to the AE events generated due to friction among pre-existing crack interfaces. Details of the discussion can be found in reference [9].

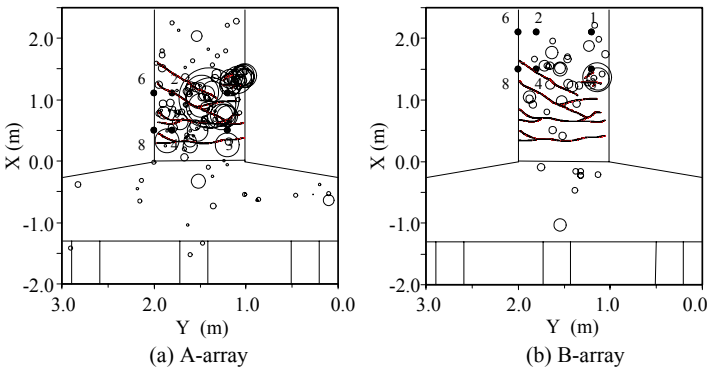

Fig. 6 3D AE sources in RC-pier. Sources were obtained from 10 times (a) and 4 times train passages (b).

Fig. 6 shows 3D source locations in case of RC-pier, where all sources are projected to the north side and the scale of the circle reflects the averaged peak amplitude of all hits contributing to the AE source/event. Here the scale of AE sources is only focused because of different population parameters of train passages. A-array shows many AE sources generated actively around the observed cracks, and the scale of AE sources distributed widely, namely from small to large magnitude. While in B-array, the large scale of AE sources as that in A-array could not be derived, but almost the same scale of AE sources were presented.

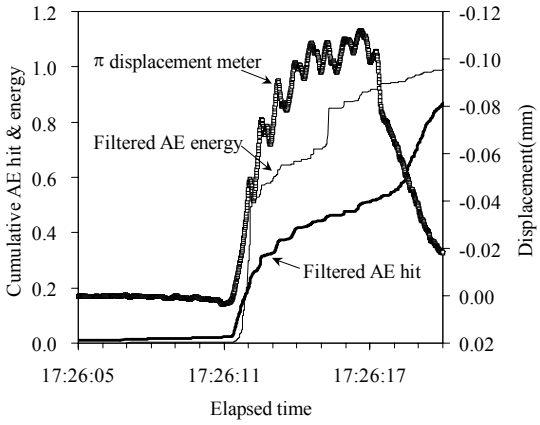

Fig. 7 Both activities of AE and displacement.

4.2 AE activity due to train passage

To determine the RTRI and Calm ratio, it is essential to obtain AE activity as a function of external parameter such as displacement. Fig. 7 shows in case of C-pier, where cumulative AE activity and behavior of π-displacement meter, installed on the observed crack, are drawn with elapsed time. In the chart, both activities of AE hit and AE energy are shown. To evaluate AE events only, which is attributed to the secondary AE activity, a high pass filter of 20 kHz was performed to the raw AE data set. Even for the filtered both parameters, different trends could be observed not only at their onset time but at the time when they showed sudden increase. Additionally, a maximum value of π-displacement meter, which is essential to obtain the RTRI, was readily identified with the chart in C-pier (see 17:26:17 in Fig. 7).

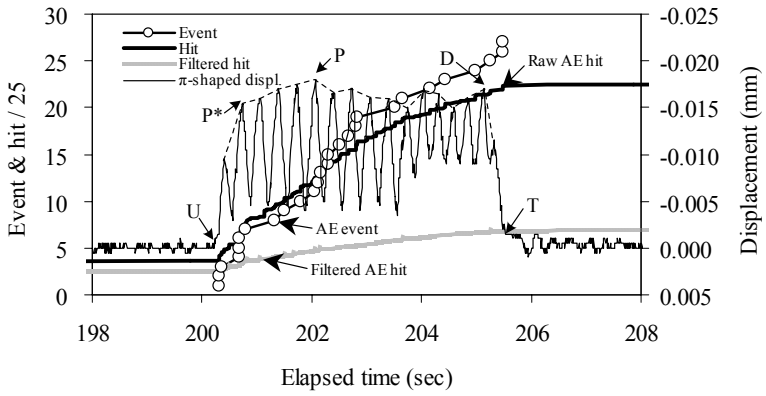

Fig. 8 Both activities with a train passage of bullet train.

In RC-pier, behavior of AE activity and π-displacement meter are given in Figure 8. The displacement did not show the monotonic behavior but showed cyclic behavior when passing the bullet train. This is attributed to the cars attaching to the bullet train, suggesting the difficulty in obtaining the both of Calm ratio and RTRI. In this paper for the displacement for RC-pier, the envelope of the variation was used with reference to the AE activity (details can be seen in discussion).

4.3 RTRI & Calm ratio

Based on the detected AE activity and the measurement of the π-displacement meter, the damage degree of C-pier is quantified using the RTRI and Calm ratio (see Fig. 9). The AE activity of raw data is denoted with open circles (hit) and open triangles (energy), whereas that extracted with the high pass filtering is exhibited by solid circles (hit) and solid triangles (energy). Dotted lines in the chart show reported criteria with regard to damage levels [2]. It is noted that raw AE activity is mainly caused by the train movement but filtered data presents the emissions induced by the crack movement [9]. The RTRI shows smaller value than 0.2 in the filtered AE activity, implying that in case of seriously damaged structures, AE events within the material were started to be generated with a slight movement of the structure, namely from smaller displacement. A different trend can be found in the Calm ratio. Smaller Calm ratios were both obtained in the raw and filtered AE activity, whereas larger were

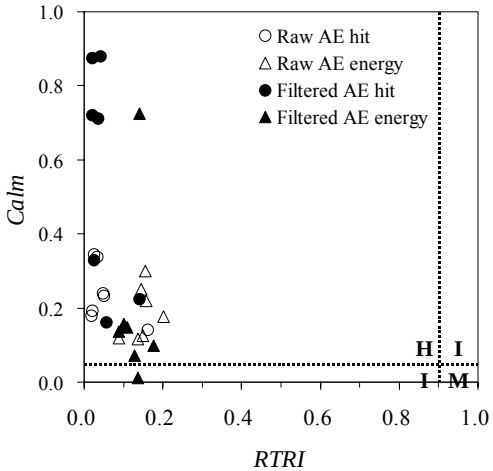

Fig. 9 Calm ratio and RTRI in C-pier, showing H: heavily damage, I: intermediately damage and M: moderately damage.

additionally observed in the filtered AE hits, suggesting that the number of AE hit during the loading process almost equals to the number of AE hit during the unloading process in the filtered activity (see about 0.8 in Calm ratio). It should be noted, however, the filtered AE energy showed smaller value than 0.2 in contrast to the filtered AE hits. This implies that the AE hits during the unloading process featured very small scale of energy in comparison to those during the loading process. Thus in C-pier, it can be concluded that RTRI is potentially applied for damage evaluation but it should be considered that the Calm ratio depends strongly on the used AE parameter.

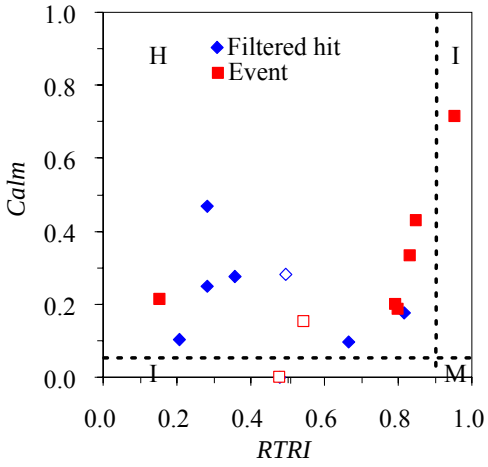

Fig. 10 Calm ratio and RTRI in RC-pier, where 'Event' stands a located source.

Fig. 10 shows those in case of RC-pier in the same manner as in Fig. 9. The solid symbol denotes the case of A-array and the open symbol represents the case of B-array. Each distribution of filtered hit and events shows a different trend. In the RTRI, B-array shows almost 0.5, however, A-array distributed two regions as smaller than 0.4 and larger than 0.6. In the Calm ratio, B-array shows smaller than 0.3, whereas A array widely distributed from 0.1 to 0.7. In the RC-pier, damage quantification was thus difficult with Calm ratio and RTRI.

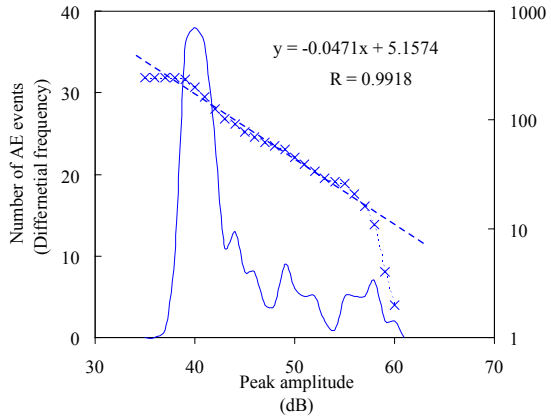

Fig. 11 Amplitude distributions in C-pier.

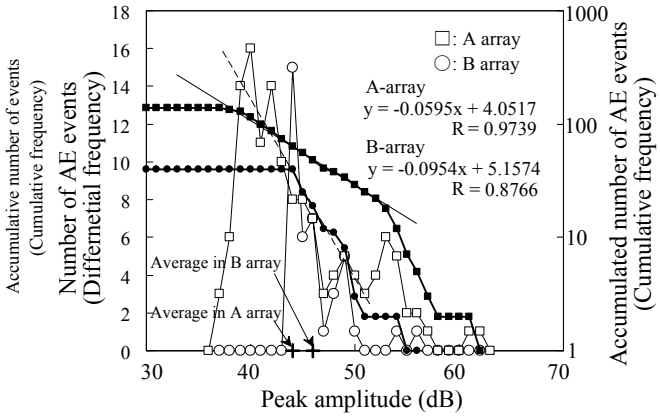

Fig. 12 Amplitude distribution in RC-pier.

4.4 Improved b-value

Fig. 11 shows the amplitude distribution of C-pier. A line shows the differential type of distribution and a cross symbol shows the cumulative type of distribution. In the chart, the result of I*b*-value analysis is indicated by the broken line as well, where a negative gradient of the line denotes the I*b*-value of about 0.05. In C-pier, since a shear type of macroscopic crack was observed, it should be recognized that the I*b*-value corresponding to the critical damage is about 0.05.

The same AE peak amplitude distributions of RC-pier as in Fig. 11 are exhibited as in Fig. 12. Open circles (B-array) and open squares (A-array) show the differential type of distribution and solid symbols show the cumulative type of distribution. In the figure, the averages of peak

amplitudes in both arrays from all derived AE events are indicated with cross symbols as well. Again A-array corresponds to seriously damaged state while B-array shows the intermediately damaged state. The figure shows that the average of peak amplitude in B-array appeared larger value than that in A-array, suggesting that AE events generated from the intermediately damaged state had a larger value than seriously damaged state. Since, in general, the larger the scale of fracture becomes, the larger the AE peak amplitude has, the fact of the averages of peak amplitude does not suffice the general idea. In the differential type of distribution in B-array, AE events distributed narrowly around 45 dB, and AE events of larger than 50 dB did not appear so much, whereas it distributed widely from small scale to large scale (see around 40 dB and 55 dB) in A-array. The difference of the range in the distribution resulted in thus the antithesis of general ideal. Solid plots show that the gradient in A-array (= 0.06) appeared smaller value than that in B-array (= 0.10), implying that the improved *b*-value becomes smaller with damage evolution. Moreover, considering the I*b*-value obtained from C-pier, I*b*-value of around 0.05 might suggest the seriously damaged condition of the structures.

5. Discussion

5.1 Damage quantification with RTRI and Calm ratio

As shown in Figs. 7 and 8, both, AE activity and external parameters as displacement should be prepared to obtain the RTRI and Calm ratio. In Fig. 8, however, considerably varied behavior with up and down movement was observed when passing bullet trains, moreover even when conventional trains passed, the same manner of cyclic behavior was still confirmed (see Fig. 7). This suggests that when searching the corresponding value with onset of AE activity, for example, it should be carefully treated during unloading processes. Such attention also should be paid even during uploading processes: the displacement value corresponding to the onset of AE activity showed smaller value than previously during a series of loading process, namely ‘one’ train passage. Furthermore, it is also important to decide the maximum value during the loading process, particularly for obtaining Calm ratio. In Fig. 9, Calm ratios were obtained on the basis of Fig. 8 using the following cumulative AE activity: AE events were accumulated between U and P for the loading process, while for the unloading process, those between D and T were accumulated. This is a finally employed idea to decide AE activity both during loading and unloading processes i.e., accumulation of AE events during the uploading was firstly tried between U and P*, however, many cases showed no AE events in such condition at all. This suggests that it is crucially important to decide the term both of loading (up-lading) and unloading (down-loading) processes in obtaining the Calm ratio.

Not only for Calm ratio (see Figs. 9 and 10) but also RTRI (see Fig. 10), damage quantification depending on the damage level was difficult to find, and therefore further studies should be needed to clarify the applicability of those damage indices for actually damaged structures as well as considering the load/unload definition mentioned above.

5.2 Damage evaluation using improved b-value

Improved *b*-values showed 0.05 in case of seriously damaged structures (see Fig. 11 and A-

array in Fig. 12), while in intermediately damaged, *b*-value of about 0.1 were obtained. As mentioned, it is difficult to identify the damage degree with peak amplitude only (more details of discussion can be found in [10]), and the analysis of improved *b*-value does not need such external parameters as displacement. This leads a conclusion that I*b*-values can suggest damage condition reasonably although more applications with a variety of damage levels should be collected systematically.

6. Conclusions

Main findings obtained through the study can be summarized as follows:

1) In RTRI and Calm ratio, obtained from AE activity with reference to structural deformation, they were strongly dependent both on the definition of loading processes, namely loading and unloading, and an AE parameter employed. Thus, much more applications with a variety of fracture types and levels should be needed to clarify the applicability as a damage index.
2) It was difficult to associate damage levels with AE peak amplitudes, the peak amplitude distribution showed characteristic trends depending on the damage levels, in especial, improved b-value, showing a gradient of the distribution, would be a promising parameter providing damage degree quantitatively.

References

1) The Japanese Society for Non-Destructive Inspection: Recommended practice for in situ monitoring of concrete structures by acoustic emission, NDIS2421, p. 24, 2000.

2) Ohtsu, M., M. Uchida, T. Okamoto and S. Yuyama, Damage assessment of reinforced concrete beams quantified by acoustic emission, ACI Structural Journal Vol. 99, No. 4, pp.411-417, 2002.

3) Fowler, T.J., Experience with acoustic emission monitoring of chemical process industry vessels, Progress in Acoustic Emission III, JSNDI, pp. 150-162, 1986.

4) Yuyama, S., T. Okamoto, M. Shigeishi, M. Ohtsu and T. Kishi, A proposed standard for evaluating structural integrity of reinforced concrete beams by AE, Acoustic Emission: Standards and Technology Update, ASTM STP1353, pp. 25-40, 1998.

5) Shiotani, T., M. Shigeishi and M. Ohtsu, Acoustic emission characteristics of concrete-piles, Construction and Buildings Materials, Vol. 13, Elsevier Science Ltd., pp. 73-85, 1999.

6) Luo, X., H. Haya, T. Inaba, T. Shiotani and Y. Nakanishi, Experimental study on evaluation of breakage in foundations using train-induced acoustic emission, Proc. Structural Engineering World Congress 2002, Paper No. T9-1-e-3, 2002.

7) Shiotani, T., K. Fujii, T. Aoki and K. Amou, Evaluation of progressive failure using AE sources and improved *b*-value on slope model test, Progress in Acoustic Emission VII, JSNDI, pp. 529-534, 1994.

8) Shiotani, T. and M. Ohtsu, Prediction of slope failure based on AE activity, Acoustic Emission: Standards and Technology Update, ASTM STP 1353, pp. 156-172, 1999.

9) Shiotani, T., Y. Nakanishi, X. Luo, H. Haya and T. Inaba, Evaluation of structural integrity in railway structures using train-induced acoustic emission, Structural Faults & Repair 2003 (CD-ROM), Engineering Technics Press, 2003.

10) Shiotani, T., X. Luo, H. Haya and M. Ohtsu, Damage quantification for concrete structures by improved *b*-value analysis of AE, 11th International Conference on Fracture, submitted.